Proceedings of the ASME 2020
Dynamic Systems and Control Conference
DSCC2020
October 5-7, 2020, Virtual, Online

DSCC2020-3221

ERROR DYNAMICS DESIGN VIA A REPETITIVE LOOP FOR UDE-BASED ROBUST CONTROL TO REJECT PERIODIC DISTURBANCES

Yeqin Wang[1,2]*, **Yiting Dong**[3], **and Jiguo Dai**[3]
[1]National Wind Institute, Texas Tech University
Lubbock, TX 79409
[2]Syndem LLC, Willowbrook, IL, 60527

Beibei Ren[3], **and Qing-Chang Zhong**[4]
[3]Department of Mechanical Engineering
Texas Tech University, Lubbock, TX 79409
[4]Department of Electrical and Computer Engineering
Illinois Institute of Technology, Chicago, IL 60616

ABSTRACT

The uncertainty and disturbance estimator (UDE)-based robust control has a two-degree-of-freedom nature through the design of the error dynamics and the design of the UDE filters. In the conventional design to handle periodic disturbances or mixed sinusoidal disturbances, high-order UDE filters incorporated with the internal model principle (IMP) or time-delay filters (TDF) are adopted to achieve the asymptotic reference tracking and the asymptotic disturbance rejection. In this paper, a new error dynamics design combined with a repetitive loop is proposed for the UDE-based robust control to achieve the asymptotic rejection of both step disturbances and periodic disturbances. The disturbance rejection performance is investigated through the two-degree-of-freedom nature, and the practical implementation of the proposed design is illustrated to eliminate the infinite bandwidth of the repetitive loop. The proposed design is validated through the simulation studies of a battery charging system with comparison to different reported designs of the conventional UDE-based robust control.

Keywords: Rejection of periodic disturbances, error dynamics design, repetitive loop, uncertainty and disturbance estimator (UDE).

INTRODUCTION

Engineering signals usually include periodic signals or mixed multi-frequency sinusoidal signals. In the control system design, in order to deal with these signals, particularly from the disturbances, and to achieve the asymptotic reference tracking, one possible solution is through the internal model principle (IMP) design. Based on the idea of the IMP, a repetitive control (RC) method is proposed in [1] to handle periodic reference commands or periodic disturbance inputs. In order to improve the robustness of the RC, the infinite dimensional structure in the RC can be modified via adding a low pass filter in [1] or a real-rational, stable single-input-single-output (SISO) transfer function in [2]. Moreover, a slight time delay is introduced in the period parameter of the RC to further improve the performance [2]. Later, the RC is discretized for the implementation in the digital controllers in [3]. Nowadays, the RC technique has been widely used in various control systems, such as servo motor control in [4], power electronics control in [5,6], and laser-based additive manufacturing in [7].

On the other hand, a robust control method, the uncertainty and disturbance estimator (UDE)-based control, is proposed in [8] to handle uncertainties and disturbances as a replacement of the time delay control (TDC) in [9], where measuring the derivative of the states is avoided, compared to the TDC. The UDE-based robust control is based on the assumption that a signal can be approximated and estimated through a filter with the proper bandwidth. Hence, it is able to quickly estimate uncertainties and disturbances and provide the outstanding robust performances. In recent years, the UDE-based robust control has demonstrated excellent performances in broad practical applications [10–13]. In addition, the theoretical extensions of the UDE-based robust control are further investigated in many studies. In [14], the two-

*Contact author: yeqin.wang.1987@ieee.org

degree-of-freedom nature with both error dynamics design and filter design of the UDE-based robust controller is analyzed to guide the parameter selections. The tradeoff between the reference tracking and disturbance rejection under finite bandwidth constraints in the UDE-based controller is investigated in [15]. The output feedback design of the UDE-based robust control is investigated in [16] with limited plant information, where an equivalent system consisting of a first-order linear system plus a lumped uncertain term is used to represent the general class of nonlinear SISO systems. Particularly, in order to achieve asymptotic reference tracking and disturbance rejection, different filter deigns are investigated to improve the performance of the UDE-based robust control based on the two-degree-of-freedom nature. For example, in [17], the filter design based on the IMP is investigated with multi-frequency components targeted to reject mixed sinusoidal disturbances. A time-delay filter (TDF) combined with a low pass filter is adopted in [18] to handle nonlinear loads in power electronics control subjected to multi-frequency disturbances. However, in practice, the high-order filter design might increase the difficulty of the discrete implementation for the UDE-based robust control.

The two-degree-of-freedom nature of the UDE-based robust control provides another option for the error dynamics design. For example, instead of the traditional linear design of the error dynamics, a nonlinear design with the time-varying gain is investigated in [19] to handle both the input constraint and the integral windup. In this paper, a new error dynamics design based on a repetitive loop is proposed for the UDE-based robust control to handle periodic disturbances or mixed sinusoidal disturbances. The disturbance rejection performance for both step disturbances and periodic disturbances is investigated through the two-degree-of-freedom nature of the modified UDE-based robust control, and the practical implementation of the proposed design is provided to eliminate the infinite bandwidth of the repetitive loop. Compared to the filter designs investigated in [17, 18] for the rejection of periodic disturbances or sinusoidal disturbances, the proposed design has a simple structure that can be implemented easily. And the simulation studies of a battery charging system are provided to validate the proposed design with comparison to the conventional UDE-based robust control [8] and different filter designs in [17].

1 Overview of the UDE-based Robust Control with Two-degree-of-freedom Nature

Consider the following first-order SISO plant

$$\dot{x} = ax + f(x,u) + bu + d(t) \tag{1}$$

where $x \in R$ is the system state, a is a known constant, $f(x,u) \in R$ is the unknown system dynamics, b is a known non-zero constant, $u \in R$ is the system input, and $d(t) \in R$ is the bounded external disturbance. The unknown system dynamics and external disturbance can be lumped into an uncertain term

$$u_d(t) = f(x,u) + d(t).$$

Therefore, the original system can be represented as

$$\dot{x} = ax + bu + u_d(t)$$

and its corresponding system in the frequency domain can be obtained as

$$sX(s) = aX(s) + bU(s) + U_d(s) \tag{2}$$

where the Laplace transformation of a signal is denoted by the corresponding capital letter. A reference model is given to generate a reference trajectory with a desired performance

$$sX_m(s) = -a_m X_m(s) + b_m C(s) \tag{3}$$

where $X_m(s) \in \mathbb{R}$ is the reference state; $a_m > 0$, $b_m > 0$ are the reference system parameters; and $C(s)$ can be a piecewise continuous and uniformly bounded command signal. In the UDE-based robust control, the control objective is to make the system state $X(s)$ asymptotically track the desired reference trajectory $X_m(s)$. Therefore, a desired error dynamics is designed as

$$sE_x(s) = -(a_m + k)E_x(s) \tag{4}$$

with the tracking error defined as $E_x(s) = X_m(s) - X(s)$, where $(a_m + k) > 0$ is the error feedback gain.

Combining (2)-(4), the control law $U(s)$ can be obtained as

$$\begin{aligned} U(s) = \frac{1}{b}\big[&-aX(s) - a_m X_m(s) + b_m C(s) \\ &+ (a_m + k)E_x(s) - U_d(s)\big] \end{aligned} \tag{5}$$

and the lumped uncertain term $U_d(s)$ can be represented as

$$U_d(s) = sX(s) - aX(s) - bU(s). \tag{6}$$

Following the procedures in [8], $U_d(s)$ can be approximated by a filter $G_f(s)$ with

$$\hat{U}_d(s) = G_f(s)U_d(s) = G_f(s)\left[sX(s) - aX(s) - bU(s)\right] \tag{7}$$

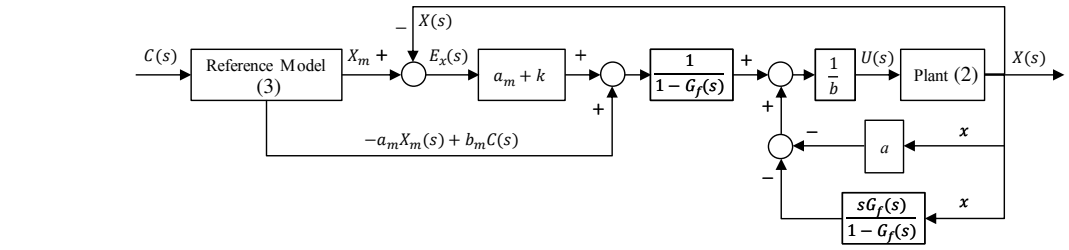

(a) Conventional UDE-based robust control

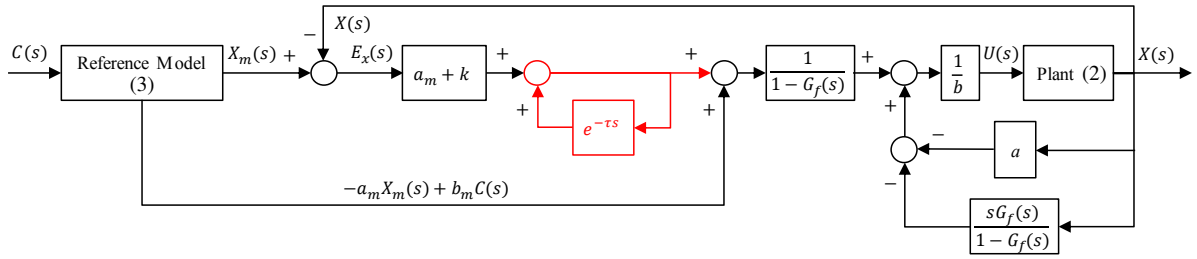

(b) Proposed modified UDE-based robust control based on the new error dynamics with a repetitive loop

FIGURE 1. The scheme of the conventional UDE-based robust control and the proposed modified UDE-based robust control.

where $G_f(s)$ is the UDE filter with both a strictly proper stable manner and an appropriate bandwidth to cover the spectrum of $U_d(s)$. Replacing $U_d(s)$ with $\hat{U}_d(s)$ in (5), there is

$$U(s) = \frac{1}{b}\{-aX(s) - a_m X_m(s) + b_m C(s) + (a_m + k)E_x(s) - G_f(s)[sX(s) - aX(s) - bU(s)]\}. \quad (8)$$

Then, the final UDE-based robust control law can be formulated as

$$U(s) = \frac{1}{b}\left\{-aX(s) - \frac{sG_f(s)}{1 - G_f(s)}X(s) + \frac{1}{1 - G_f(s)}[-a_m X_m(s) + b_m C(s) + (a_m + k)E_x(s)]\right\}. \quad (9)$$

The scheme of the conventional UDE-based robust control is shown in Fig. 1(a).

Substituting (9) into (2), different from the desired error dynamics (4), the actual error dynamics becomes

$$sE_x(s) = -(a_m + k)E_x(s) + [G_f(s) - 1]U_d(s). \quad (10)$$

Then the final tracking error $E_x(s)$ is obtained as

$$E_x(s) = \frac{1}{s + (a_m + k)}U_d(s)[G_f(s) - 1]. \quad (11)$$

In order to achieve the asymptotic reference tracking and eliminate the tracking error, specifically to handle the lumped uncertain term $U_d(s)$, there are two-degree-of-freedom designs: one is through the design of the error dynamics feedback gain $a_m + k$ in (4), the other is through the filter design $G_f(s)$ to eliminate the estimation error $\tilde{U}_d(s)$ of the lumped uncertain term

$$\tilde{U}_d(s) = U_d(s)[G_f(s) - 1]. \quad (12)$$

Then, the actual error dynamics of the conventional UDE-based robust control with the two-degree-of-freedom nature becomes

$$E_x(s) = \frac{1}{s + (a_m + k)}\tilde{U}_d(s). \quad (13)$$

In order to achieve good disturbance rejection, specifically for periodic disturbances or sinusoidal disturbances, the filter design based on the IMP is investigated in [17], and a TDF is adopted in [18]. In [17], if the disturbances with mixed multi-frequency sinusoidal signals are considered, the high-order filters are required to handle all frequency components. The TDF developed in [18] needs to combine with a low-pass filter for the practical realization. However, the high-order filter designs might increase the difficulty of the practical implementation for the UDE-based robust control in real applications, because the UDE filter appears in both the numerator and denominator of the UDE-based robust control law (9), as shown in Fig. 1(a).

2 Error Dynamics Design with a Repetitive Loop

In order to achieve the asymptotic reference tracking and eliminate the tracking error, instead of the filter design, a new

error dynamics based on a repetitive loop is proposed for the UDE-based robust control to handle periodic disturbances. The disturbance rejection performance for both step disturbances and periodic disturbances is further analyzed. How to carry out a practical implementation is also provided to eliminate the infinite bandwidth of the repetitive loop.

2.1 Control Design

Instead of the error dynamics in equation (4), a new error dynamics with a repetitive loop is designed as

$$sE_x(s) = -\frac{a_m + k}{1 - e^{-\tau_d s}} E_x(s) \tag{14}$$

where τ_d is a time constant, which should be designed according to the frequency spectrum of the lumped uncertain term $U_d(s)$.

Following the similar procedures of the conventional UDE-based robust control in Section 1, the modified UDE-based robust control law can be obtained as

$$\begin{aligned} U(s) = \frac{1}{b}\Bigg\{ & -aX(s) - \frac{sG_f(s)}{1 - G_f(s)} X(s) \\ & + \frac{1}{1 - G_f(s)} \Bigg[-a_m X_m(s) \\ & + b_m C(s) + \frac{a_m + k}{1 - e^{-\tau_d s}} E_x(s) \Bigg] \Bigg\}. \end{aligned} \tag{15}$$

The scheme of the proposed modified UDE-based robust control is shown in Fig. 1(b). Compared to the conventional UDE-based robust control in [8], shown in Fig. 1(a), it can be seen that only a time-delay feedback loop is added to the error term $(a_m + k)E_x(s)$ in the proposed modified UDE-based robust control.

Substituting (15) into (2), it can be achieved that

$$sE_x(s) = -\frac{a_m + k}{1 - e^{-\tau_d s}} E_x(s) + \tilde{U}_d(s) \tag{16}$$

then, the new actual error dynamics with the similar two-degree-of-freedom nature for the proposed modified UDE-based robust control (15) is obtained as

$$E_x(s) = \frac{1 - e^{-\tau_d s}}{s - s e^{-\tau_d s} + a_m + k} \tilde{U}_d(s). \tag{17}$$

The Bode diagrams for the transfer functions of both the conventional actual error dynamics (13) and the new actual error dynamics (17) with $a_m + k = 100\pi$ and $\tau_d = 0.05$ are shown in Fig. 2. They show that the magnitudes of both curves are far below 0 dB, and the phases of both curves are far beyond -180^o. This indicates that both (13) and (17) have large positive phase margins (PM) and the infinite gain margins (GM). Therefore, both the original actual error dynamics (13) and the new actual error dynamics (17) can provide the stable convergence of the tracking errors in the UDE-based robust control framework. In addition, the Bode diagrams for the transfer function of the new actual error dynamics (17) with different time constants τ_d are illustrated in Fig. 3. It can be seen that their maximum magnitudes are always below -44 dB, and the phases are always remained between -90° and $+90^\circ$ with different τ_d, which can make sure the stable convergence of the tracking errors.

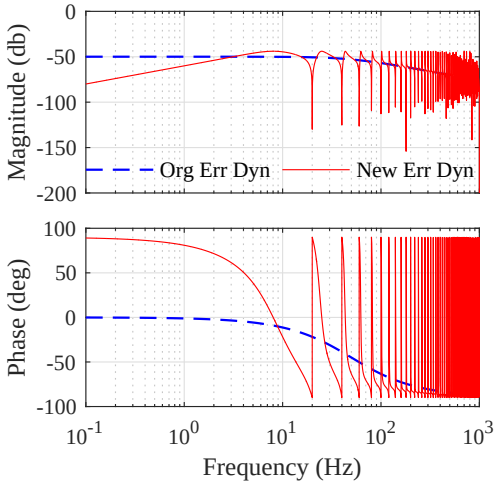

FIGURE 2. The Bode diagrams for the transfer functions of the conventional actual error dynamics (13) and the new actual error dynamics (17).

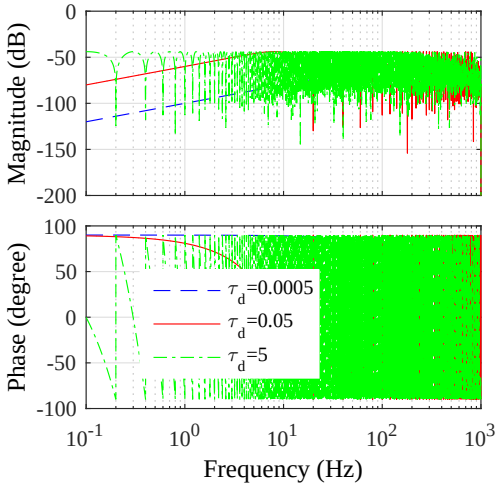

FIGURE 3. The Bode diagrams for the transfer function of the new actual error dynamics (17) with different time constants τ_d.

In the above design, the first-order SISO system is considered. The proposed control can be extended to high-order systems in future work, e.g., with the combination of the output feedback design technique [16].

2.2 Performance analysis for disturbance rejection

In order to analyze the disturbance rejection performances, the new actual error dynamics (17) can be rewritten as

$$E_x(s) = \frac{(1-e^{-\tau_d s})\left[G_f(s)-1\right]U_d(s)}{s-se^{-\tau_d s}+a_m+k}. \tag{18}$$

As an engineering signal, the lumped uncertain term $U_d(s)$ might includes step signals and periodic signals or mixed sinusoidal signals. If the UDE filter $G_f(s)$ is designed as a low-pass filter with $G_f(0)=1$, then

$$G_f(s)-1=0$$

and

$$\frac{(1-e^{-\tau_d s})\left[G_f(s)-1\right]}{s-se^{-\tau_d s}+a_m+k}=0$$

when $s=0$. This indicates that the step part of the uncertain term $U_d(s)$ can be handled through the low-pass filter $G_f(s)$.

In order to handle periodic signals or mixed sinusoidal signals in the lumped uncertain term $U_d(s)$, the time constant τ_d in the new error dynamics (14) should be well designed. For example,

$$\tau_d = \frac{1}{f_d}$$

where τ_d is the common period of the periodic signals, or f_d is the common frequency of all sinusoidal signals in the lumped uncertain term $U_d(s)$. Normally, the minimal common period or maximal common frequency can be selected. In this way, when $s=\pm 2\pi f_d j$,

$$1-e^{-\tau_d s}=0$$

and

$$\frac{(1-e^{-\tau_d s})\left[G_f(s)-1\right]}{s-se^{-\tau_d s}+a_m+k}=0.$$

This means that the periodic part of the lumped uncertain term $U_d(s)$ can be handled through the repetitive loop in the error dynamics design.

With both the step and periodic parts of the lumped uncertain term $U_d(s)$ effectively rejected through the two-degree-of-freedom design, the tracking error can converge to zero finally. It is worth noting that the UDE filter $G_f(s)$ can be simply selected as a first-order low pass filter in the proposed design with

$$G_f(s) = \frac{\omega_0}{s+\omega_0} \tag{19}$$

then $\frac{1}{1-G_f(s)} = 1+\frac{\omega_0}{s}$ and $\frac{G_f(s)}{1-G_f(s)} = \omega_0$. Compared to the UDE filter $G_f(s)$ design based on the IMP in [17] or the combination of TDF with a low pass filter in [18], the proposed design is convenient for the practical discrete implementation.

2.3 Practical implementation

The proposed design in (14) is characterized by an infinite bandwidth, as illustrated in Fig. 2, which might cause some issues during the practical applications, as discussed in [2, 18]. It should be modified as

$$sE_x(s) = -\frac{a_m+k}{1-W(s)e^{-(\tau_d-\triangle\tau)s}}E_x(s) \tag{20}$$

where $W(s)$ is a real-rational, stable SISO transfer function with $\|W(s)\|_\infty \le 1$, as illustrated in [2], and $\|W(s)\|_\infty$ denotes the infinity norm of $W(s)$. $\triangle\tau$ is the delay term caused by $W(s)$. A

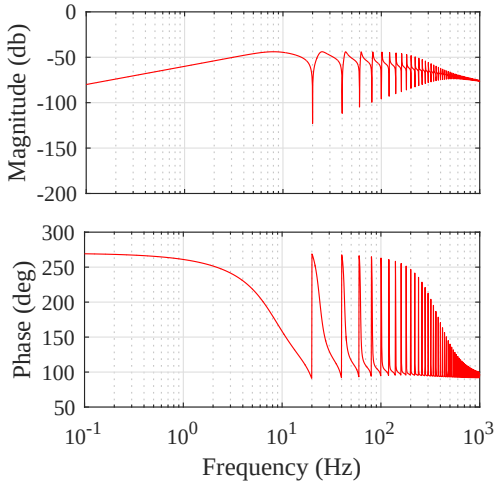

FIGURE 4. The Bode diagram for the transfer function of the new actual error dynamics with the practical implementation (24).

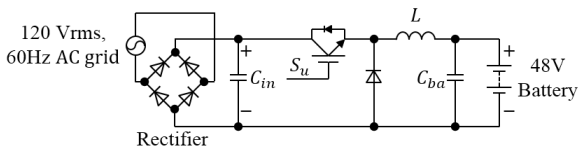

FIGURE 5. A battery charging system.

simple choice of $W(s)$ is a low pass filter, for example,

$$W(s) = \frac{1}{\tau_r s + 1} \tag{21}$$

and the corresponding $\triangle\tau$ can be designed as

$$\triangle\tau = \tau_d \tan^{-1}(\frac{\tau_r}{\tau_d}). \tag{22}$$

Normally, $\tau_r \ll \tau_d$, hence, $\triangle\tau$ can be approximated as

$$\triangle\tau \approx \tau_r. \tag{23}$$

More information about the $\triangle\tau$ design for different $W(s)$ can be found in [18]. Usually, a very large bandwidth of $W(s)$ can be selected in practical applications, but should be within the sampling frequency of the digital controllers. It is worth noting that the practical implementation by adding the $W(s)$ term does not complicate the proposed modified UDE-based robust control design too much, because the $e^{-\tau s}$ term in Fig. 1(b) can be simply replaced by $W(s)e^{-(\tau_d - \triangle\tau)s}$.

Through the modification of (20), the new actual error dynamics (17) becomes

$$E_x(s) = \frac{1 - W(s)e^{-(\tau_d - \triangle\tau)s}}{s - sW(s)e^{-(\tau_d - \triangle\tau)s} + a_m + k} \tilde{U}_d(s). \tag{24}$$

The corresponding Bode diagram is show in Fig. 4 with $a_m + k = 100\pi$, $\tau_d = 0.05$, $W(s) = \frac{2000\pi}{s+2000\pi}$ and $\triangle\tau = \frac{1}{2000\pi}$. It can be noticed that the infinite bandwidth is eliminated by $W(s)$. With the compensation of the delay term $\triangle\tau$, the same frequency components targeted to the spectrum of the disturbances within the bandwidth of $W(s)$ still can hold, compared to Fig. 2.

3 Simulation Studies

In order to verify the proposed modified UDE-based robust control design, a battery charging system, as shown in Fig.5, is built for the simulation studies. The main part of this battery-charging system is a buck DC/DC converter, where the output side is a 48V lead-acid battery pack, and the input side is a single-phase rectifier combined with the utility-level 120 Vrms, 60 Hz AC grid. The input capacitor is $C_{in} = 1000\,\mu$F, the battery capacitor is $C_{ba} = 250\,\mu$F, and the inductor is $L = 3$ mH. There are two modes for battery charging: constant current mode and constant voltage mode. In this simulation, only the constant current mode is considered, and the battery charging current will be controlled with the reference set as 30 A. According to the output feedback design technique in [16], the input-output relationship of this battery-charging system can be modeled as

TABLE 1. Control Parameters

Parameters	Values	Parameters	Values
a	3.333	$G_f(s)$	$\frac{2000}{s+2000}$
b	50000	τ_d	$\frac{1}{120}$
a_m, b_m	100	$W(s)$	$\frac{10000\pi}{s+10000\pi}$
$a_m + k$	200	$\triangle\tau$	$\frac{1}{10000\pi}$

$$\dot{y}(t) = -ay(t) + bu(t) + u_d(t) \tag{25}$$

where $y(t)$ is the system output, which represents the battery charging current; $u(t)$ is the control input, which represents the duty cycle for the power electronic device; and the lumped uncertain term $u_d(t)$ represents the unmodeled dynamics and disturbances of this battery charging system. Because the input side of this system is a single-phase rectifier combined with the AC grid, u_d includes mixed periodic disturbances with the common frequency of 120 Hz, according to the properties of the single-phase rectifier.

The proposed modified UDE-based robust control (15) is used to control the battery charging current based on the system model (25), where the control parameters are shown in Table 1. How to choose parameters for the output feedback design, the UDE filter, and the error dynamics in the UDE-based robust control, can refer to [14, 16, 17]. In order to show the advantages of the proposed design, the conventional UDE-based robust control (9) in [8], and the UDE-based robust control with an IMP filter in [17] are also provided for comparison, where only one frequency component of 120 Hz is considered for the IMP design.

The system responses are shown in Fig. 6, including the battery charging current in Fig. 6(a), the fast Fourier transform (FFT) analysis of the battery charging current during $0.5\,\text{s} \sim 0.6\,\text{s}$ in Fig. 6(b), the duty cycle for the power electronic device in Fig. 6(c), and the capacitor voltage of the input side in Fig. 6(d). It can be noticed that all three controllers can converge to steady states quickly. Though the proposed modified UDE-based robust control needs an additional 0.2 s for the convergence compared with the conventional UDE-based robust control and the UDE-based robust control with the IMP filter, this small time slot does

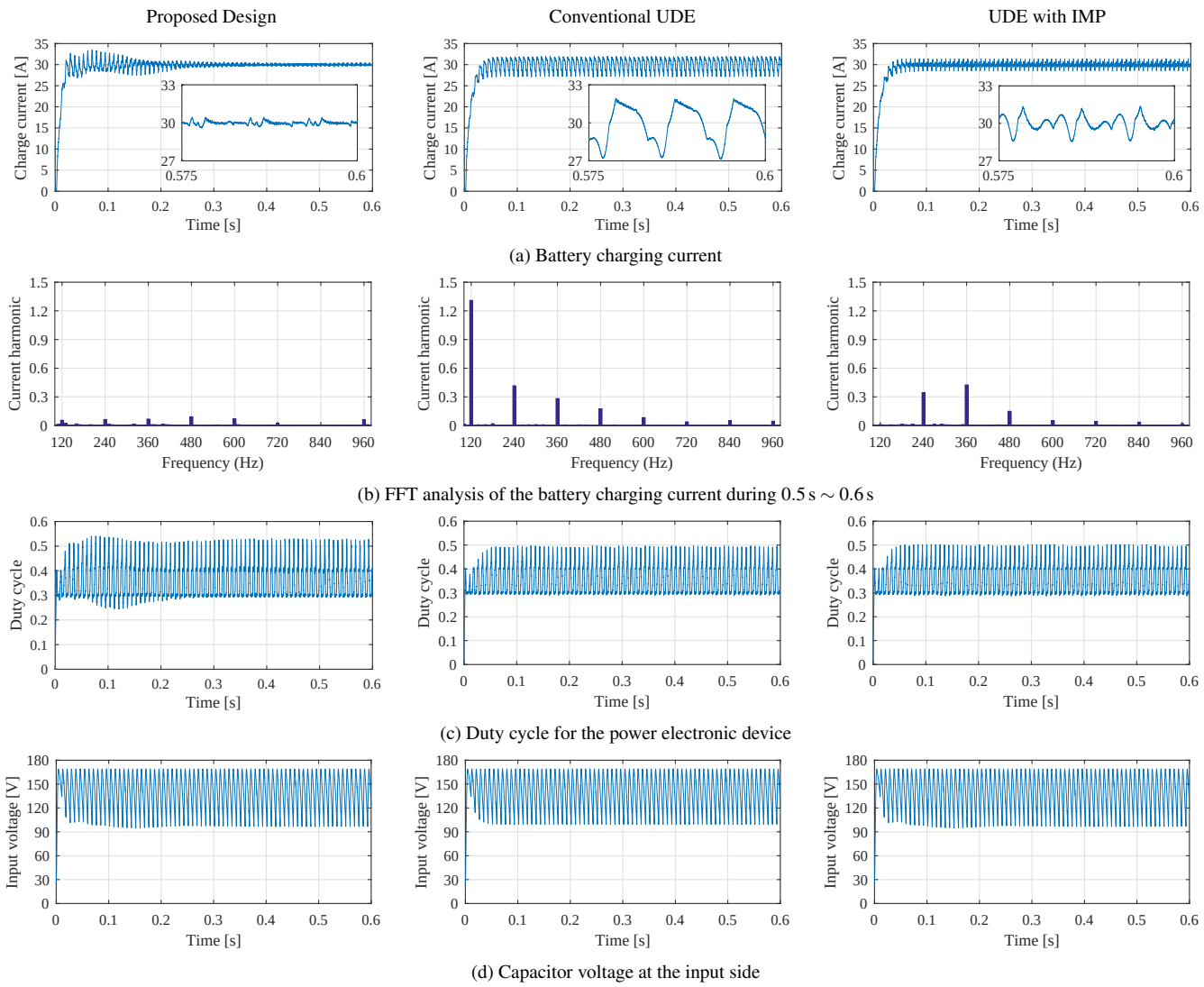

FIGURE 6. Simulation results with the proposed UDE-based robust control (left column), the conventional UDE-based robust control (middle column), and the UDE-based robust control with a single-frequency IMP filter (right column).

not affect the battery charging performance. The proposed modified UDE-based robust control can effectively reject the mixed periodic disturbances at steady state. The battery charging current only has very small oscillations, as shown in Fig. 6(a). The current harmonics within all frequency components are very small, which indicates the mixed periodic disturbances are effectively rejected, as shown in Fig. 6(b). The conventional UDE-based robust control cannot achieve the good rejection of mixed periodic disturbances with large oscillations of the battery charging current shown in Fig. 6(a), and the disturbances with all frequency components still appear in the harmonics of the battery changing current, as shown Fig. 6(b). The UDE-based robust control with the IMP filter has smaller oscillations, compared with the conventional UDE-based robust control, as shown in Fig. 6(a), but it only rejects the disturbances within the specific designed frequency of 120 Hz, as shown in Fig. 6(b). The proposed modified UDE-based robust control has a larger peak value of the duty cycle for the power electronic device than the other two controllers, as shown in Fig. 6(c), because it needs larger control efforts to reject more disturbances. The mixed periodic disturbances from the capacitor voltage of the input side are clearly indicated in Fig. 6(d). It is well known that large oscillations in the battery charging current will affect the battery performance, e.g., the degradation of the battery lifespan. The proposed modified UDE-based robust control with the new error dynamics based on the repetitive loop demonstrates better control performances than the other two controllers for this battery charging system.

4 Conclusion

In order to improve the UDE-based robust control to achieve the disturbance rejection of both step disturbances and periodic disturbances or mixed sinusoidal disturbances, this paper has explored the error dynamics design instead of the filter design to simplify the practical implementation. The new error dynamics has been proposed based on a repetitive loop. The performances of disturbance rejection have been further investigated, and the practical implementation of the proposed design has been discussed. The simulation results have validated the effectiveness of the proposed design with the comparison to different designs of the conventional UDE-based robust control.

REFERENCES

[1] Hara, S., Yamamoto, Y., Omata, T., and Nakano, M., 1988. "Repetitive control system: A new type servo system for periodic exogenous signals". *IEEE Trans. Autom. Control,* ***33***, Jul., pp. 659–668.

[2] Weiss, G., and Hafele, M., 1999. "Repetitive control of MIMO systems using H^∞ design". *Automatica,* ***35***(7), Jul., pp. 1185–1199.

[3] Grino, R., and Costa-Castello, R., 2005. "Digital repetitive plug-in controller for odd-harmonic periodic references and disturbances". *Automatica,* ***41***(1), Jan., pp. 153 – 157.

[4] Wu, M., Xu, B., Cao, W., and She, J., 2014. "Aperiodic disturbance rejection in repetitive-control systems". *IEEE Trans. Control Syst. Technol.,* ***22***(3), May, pp. 1044–1051.

[5] Hornik, T., and Zhong, Q.-C., 2011. "A current control strategy for voltage-source inverters in microgrids based on H^∞ and repetitive control". *IEEE Trans. Power Electron.,* ***26***(3), Mar., pp. 943–952.

[6] Pandove, G., and Singh, M., 2019. "Robust repetitive control design for a three-phase four wire shunt active power filter". *IEEE Trans. Ind. Informat.,* ***15***(5), May, pp. 2810–2818.

[7] Wang, D., and Chen, X., 2018. "A multirate fractional-order repetitive control for laser-based additive manufacturing". *Control Eng. Pract.,* ***77***, Aug., pp. 41 – 51.

[8] Zhong, Q.-C., and Rees, D., 2004. "Control of uncertain LTI systems based on an uncertainty and disturbance estimator". *ASME Trans. J. Dyn. Sys. Meas. Control,* ***126***(4), Dec., pp. 905–910.

[9] Youcef-Toumi, K., and Ito, O., 1990. "A time delay controller for systems with unknown dynamics". *ASME Trans. J. Dyn. Sys. Meas. Control,* ***112***(1), Mar., pp. 133–142.

[10] Ren, J., Ye, Y., Xu, G., Zhao, Q., and Zhu, M., 2017. "Uncertainty-and-disturbance-estimator-based current control scheme for PMSM drives with a simple parameter tuning algorithm". *IEEE Trans. Power Electron.,* ***32***(7), Jul., pp. 5712–5722.

[11] Ye, Y., and Xiong, Y., 2018. "UDE-based current control strategy for LCCL-type grid-tied inverters". *IEEE Trans. Ind. Electron.,* ***65***(5), May, pp. 4061–4069.

[12] Wang, Y., and Ren, B., 2018. "Fault ride-through enhancement for grid-tied PV systems with robust control". *IEEE Trans. Ind. Electron.,* ***65***(3), Mar., pp. 2302–2312.

[13] Talole, S., Chandar, T., and Kolhe, J. P., 2011. "Design and experimental validation of ude based controller–observer structure for robust input–output linearisation". *International Journal of Control,* ***84***(5), Jun., pp. 969–984.

[14] Zhong, Q.-C., Kuperman, A., and Stobart, R., 2011. "Design of UDE-based controllers from their two-degree-of-freedom nature". *International Journal of Robust and Nonlinear Control,* ***21***, Nov., pp. 1994–2008.

[15] Aharon, I., Shmilovitz, D., and Kuperman, A., 2018. "Uncertainty and disturbance estimator-based controllers design under finite control bandwidth constraint". *IEEE Trans. Ind. Electron.,* ***65***(2), Feb., pp. 1439–1449.

[16] Ren, B., Dai, J., and Zhong, Q.-C., 2019. "UDE-based robust output feedback control with applications to a piezoelectric stage". *IEEE Trans. Ind. Electron.* to be published,doi: 10.1109/TIE.2019.2941169.

[17] Ren, B., Zhong, Q.-C., and Dai, J., 2017. "Asymptotic reference tracking and disturbance rejection of UDE-based robust control". *IEEE Trans. Ind. Electron.,* ***64***(4), Apr., pp. 3166–3176.

[18] Gadelovits, S. Y., Zhong, Q. C., Kadirkamanathan, V., and Kuperman, A., 2017. "UDE-based controller equipped with a multi-band-stop filter to improve the voltage quality of inverters". *IEEE Trans. Ind. Electron.,* ***64***(9), Sept., pp. 7433–7443.

[19] Wang, Y., Ren, B., and Zhong, Q.-C., 2020. "Bounded UDE-based controller for input constrained systems with uncertainties and disturbances". *IEEE Trans. Ind. Electron.* to be published, doi: 10.1109/TIE.2020.2969069.